ICAS-88-4.10.1

FLUTTER CALCULATION OF FLUTTER MODELS FOR JAS 39 GRIPEN

Valter J. E. Stark
Saab-Scania AB, Linköping, Sweden

1 ABSTRACT

Calculated results for small and thin wing models, some of which have a launcher and missile at the tip, and for a large and likewise thin composite model with flap have been compared with test results for zero incidence. The small models were tested in a small tunnel at high-subsonic speeds and the large model in a large tunnel at transonic and low-supersonic speeds. Since the results from the calculations, which were mainly based on the linearized theory, are in good agreement with those from the carefully performed tests, it is concluded that this theory is satisfactory for flutter calculations of thin wings at zero incidence.

2 INTRODUCTION

In the development of a new aircraft, it is necessary to prove that the requirement of safety against flutter is satisfied, which implies extensive and complicated investigations. To a large part, these investigations can be performed by means of computers and computer programs.

Flutter tests in wind tunnels are needed, but alone they are not sufficient. A check by using a model of the final design is hardly possible since data are not available early enough to allow design, building, and testing of an accurately similar model. As such a model is also very expensive, it is attractive to use computer programs.

The programs must of course be checked very carefully and wind tunnel tests are required for this, but accurate simulation of the full scale design is then not necessary. A model for checking the programs and the underlying theory can accordingly be built in an inexpensive way.

It has often been said that flutter model tests are necessary because the unsteady aerodynamic forces are unreliable, but statements of this kind cannot be accepted. It has been found, namely, that errors due to other sources are equally likely. This investigation in which the accuracy of mass, stiffness, and mode data has been carefully checked, shows that flutter of thin wings at zero incidence can be predicted satisfactorily by the use of aerodynamic forces calculated by the linearized theory.

Flutter calculations for the JAS 39 Gripen were performed by the so called AEREL system in which aerodynamic routines based on the linearized theory were used. For checking this program system, several models with different complexity were built and tested. Some of the results from the calculations and tests will be shown and compared in this paper.

Recently, a finite-difference program based on the full potential equation was developed at SAAB (Ref. 1). A few results based on aerodynamic forces from this program shall be shown too.

3 WIND TUNNELS

The flutter tests to be considered were partly performed by Volvo Flygmotor AB in Sweden, called VFA in the sequel, and partly by ONERA in France.

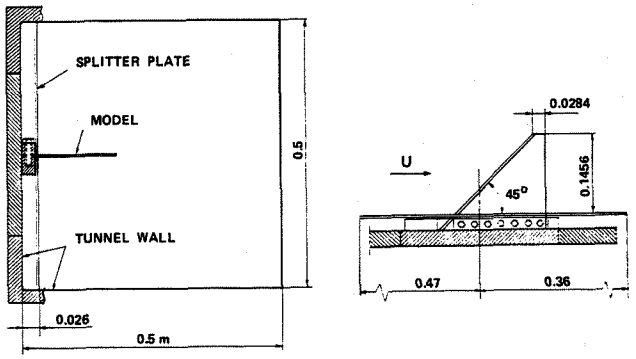

Fig. 1 Model in test section of the VFA tunnel

The tunnel employed by VFA is a comparatively small tunnel, but it offers long test runs which is required for flutter tests. It has a test section size of 0.5mx0.5m, slotted ceiling and floor, and permits transonic and supersonic tests at a maximum Reynolds number of 6x10**6 per dm.

The ONERA tests were performed in the well known S2MA tunnel at Modane.

4 MODELS

The models tested are all semi-span models which were mounted at the tunnel wall.

Six models were tested by VFA in the VFA tunnel. These models, which are small, consist mainly and simply of an aluminum plate, which is 1.48 mm thick and was clamped at the root. Some of the models, which are described and denoted as shown in Fig. 2, have a launcher and a missile model at the tip.

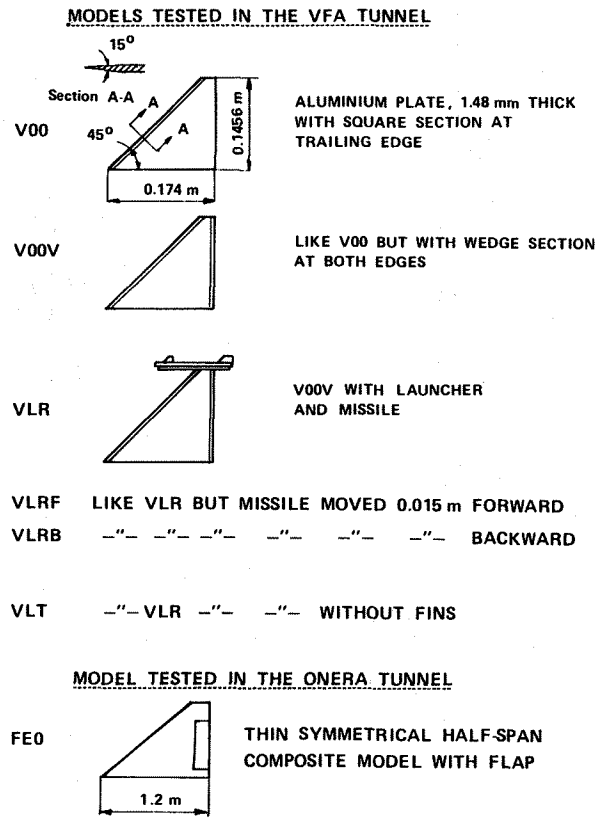

Fig. 2 Flutter models tested

The two models without launcher and missile have a span of 0.1456 m, a tip chord of 0.0284 m, and a leading edge sweep angle of 45 degrees. The first one tested, which is called V00, has a wedge shaped section at the leading edge while the other one has such a section both at the leading edge and the trailing edge.

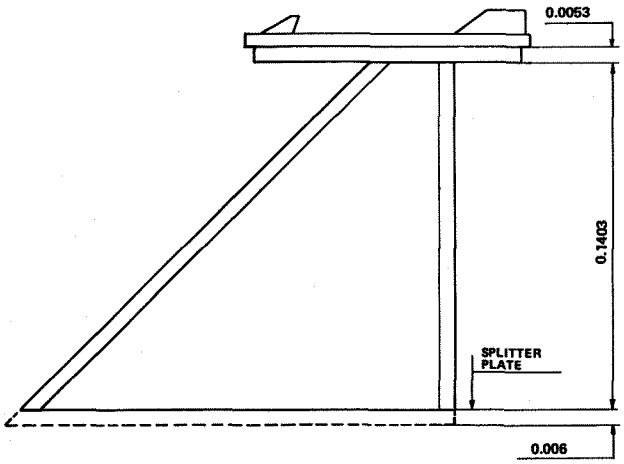

Fig. 3 Model VLR

The model configurations VLR, VLRF, VLRB, and VLT, include models of a launcher attached to the wing tip and a missile attached to the launcher. In case of VLR, the missile was attached at a nominal position, while in case of VLRF and VLRB it had a 15 mm more forward and 15 mm more backward position respectively. Fig. 3 shows VLR (with the missile fins modified as described later).

Like VLR, the model VLT includes a launcher and a missile located at the nominal position, but this missile model has no fins.

A theoretical study of the aerodynamic effects of the missile fins has been made. The three models VLRUFF, VLRUFB, and VLRUF, which were considered for this purpose, have no forward fins, no rear fins, and no fins at all respectively.

The model tested in the ONERA S2MA tunnel is a comparatively large model made from composit material (Kevlar). It was designed to be similar to the corresponding full scale surface, which implied that a comparatively large model and thus a large tunnel had to be used.

5 GROUND VIBRATION TEST TECHNIQUE

In the ground vibration tests (GVT) performed by VFA, the model was mounted at the tunnel wall in the same way as during the flutter tests.

For the small models except V00, VFA used a loudspeaker for excitation and a Laser Dopler Vibrometer for measurement of the natural modes, but for V00 as well as FE0, the impulse hammer technique (Ref. 2) was employed.

In the GVT performed by ONERA for the model FE0, this was attached to a heavy structure outside the tunnel and excited by an electro-magnetic shaker. The shaker was fed by a sinus signal and, at resonance, the response was measured by means of a portable accelerometer.

6 GVT RESULTS FOR THE SMALL MODELS

6.1 Natural Frequencies

Since only natural modes shall be used the mass, damping, and stiffness matrices are diagonal matrices. With $m(n)$, $f(n)=\omega(n)/(2\pi)$, and $\varphi(n)$ denoting the generalized mass, the natural frequency, and the damping coefficient respectively for the n:th mode, the diagonal elements of the matrices are $m(n)$, $2\alpha(n)\omega(n)m(n)$, and $m(n)\omega(n)**2$ respectively.

We want to look upon the comparisons as a check on the aerodynamic forces and have to check, therefore, that the results from the GVT for $m(n)$, $f(n)$, and the natural modes are sufficently accurate for this purpose.

The natural frequencies for simple models like V00 and V00V can be checked by calculating corresponding normalized frequencies b**2f(n)/t (b is the span and t the thickness) and comparing these to normalized frequencies for other models. The normalized frequency for thin models with the same planform is independent, namely, of the span and the thickness. The results obtained for the first three natural frequencies for the models mentioned plus some further models are given in Table 1.

Table 1 Natural and normalized frequencies for cropped delta models with aspect ratio 3.35, taper ratio 0.1616, semi-span b, tip chord c, and thickness t (b, c, and t in mm).

Model	b	c	t	f(n) n=1	2	3	b**2f(n)/t 1	2	3	Source
	73.8	14.2	0.70	151	550	785	1.18	4.28	6.11	GVT
	"	"	1.02	223	8291160		1.19	4.37	6.20	"
	147.6	28.4	0.98	52	182	269	1.16	4.05	5.98	"
	"	"	1.47	80	287	419	1.19	4.25	6.21	"
V00	151.6	"	1.48	77	277	404	1.20	4.32	6.32	"
V00V	"	"	"	77	278	399	1.20	4.34	6.25	"
VT0	"	"	1.5	77	294	408	1.17	4.50	6.25	ASKA
VT5	"	"	2.0	102	391	542	1.17	4.50	6.24	"
VT6	"	"	3.0	153	583	809	1.17	4.45	6.18	"

The first four rows contain earlier results for models of the same kind as V00, and the values in the last three rows are results from a finite-element calculation by the ASKA program using the model shown in Fig 4.

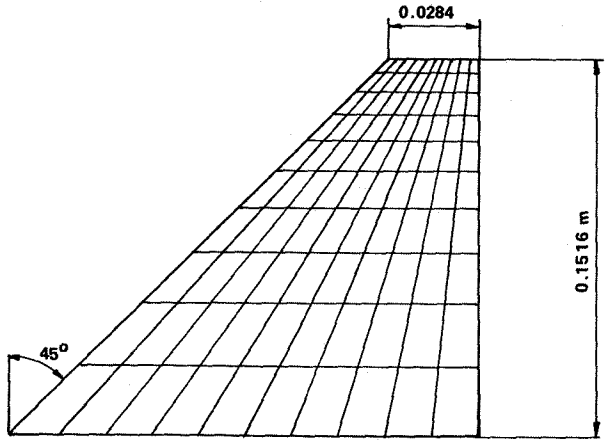

Fig. 4 Finite-element model for ASKA calculation

Since frequencies can be measured with high accuracy, it is not believed that the values obtained for f(n) are inaccurate. The small deviations of the normalized frequencies are rather thought to be due to sources such as slightly different model shape, thickness, or fastening. It is seen from the table that the finite-element calculation by ASKA gave closely agreeing results, which is encouraging.

Frequencies for the models with launcher and missile are given in Table 2 where the values in the first three rows are results from finite-element calculations. Since the mass of the launcher and missile is kept constant, the normalized frequencies cannot be expected to be independent of the thickness in this case.

Table 2 Natural and normalized frequencies for models with launcher and missile

Model	b	c	t	f(n) n=1	2	3	b**2f(n)/t 1	2	3	Source
VT2	151.6	28.4	1.5	30	86	240	0.46	1.32	3.69	ASKA
VT3	"	"	2.0	45	131	325	0.52	1.50	3.74	"
VT4	"	"	3.0	74	214	572	0.57	1.64	3.61	"
VLR	"	"	1.48	30	80	238	0.47	1.24	3.71	GVT
VLRF	"	"	"	30	78	238				"
VLRB	"	"	"	30	80	241				"
VLT	"	"	"	30	81	240				"

In spite of the large size of the elements at the root of the model (See Fig. 4), where the stresses are large and rapidly varying, the ASKA results for VT2 agree very well with those measured for VLR.

6.2 Generalized Masses

The AEREL system contains a quadrature routine which can be used for calculation of mass matrices for the simple models considered. The routine evaluates the matrix elements, which are integrals, by replacing the integrand by its value at the center of small trapezoidal elements. The elements employed in calculations for V00V are shown in Fig. 5.

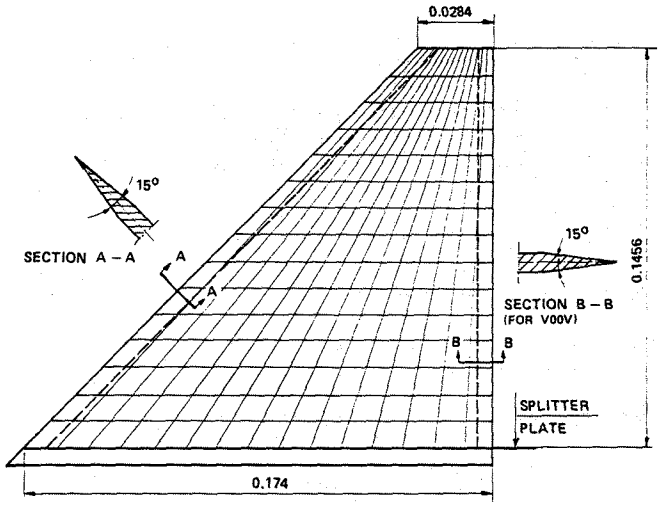

Fig. 5 Grid used for calculation of mass matrix

The calculated values of the generalized masses m(n) are given in Table 3 and compared with those measured by VFA. The upper row for each model contains the measured values and the lower row the calculated ones.

Table 3 Generalized masses (in kg)

Model	m(n)				
	n=1	2	3	4	5
V00	0.0111	0.0183	0.0145	0.0265	0.0216
	0.0073	0.0126	0.0087	0.0075	0.0121
V00V	0.0087	0.0115	0.0073	0.0098	0.0282
	0.0092	0.0117	0.0079	0.0087	0.0302
VLR	0.061	0.220	0.023	0.033	0.021
	0.061	0.208	0.023	0.027	0.020
VLRF	0.061	0.130	0.022		
	0.060	0.141	0.020		
VLRB	0.060	0.180	0.023		
	0.061	0.177	0.025		
VLT	0.060	0.200	0.023		
	0.063	0.198	0.022		

It is seen that the differences between the measured and the calculated results are significant in case of the model V00 and that these differences are small in case of the other models.

In case of V00V, the calculated complete mass matrix reads as follows:

0.0092	-0.0003	0.0001	0.0002	0.0001
-0.0003	0.0117	-0.0002	-0.0004	0.0002
0.0001	-0.0002	0.0079	0.0003	-0.0005
0.0002	-0.0004	0.0003	0.0087	0.0010
0.0001	0.0002	-0.0005	0.0010	0.0302

As the off-diagonal elements are comparatively small, and since the calculation of the mass matrix for the simple models considered should not pose any problem, it is believed that the calculated generalized masses are accurate and, accordingly, that the deviations in the case of V00 are due to experimental errors.

The close agreement for the model V00V and the models with launcher and missile is probably due to the new experimental technique that was employed for them. The generalized masses, except those for V00, were determined by measuring the change, Δf, of the natural frequency due to the addition of a small mass, Δm, to the model and estimating the limit of the ratio $\Delta m f(n) / \Delta f$ for Δm approaching zero. This ratio is plotted in Fig. 6 for the first mode of the model VLR.

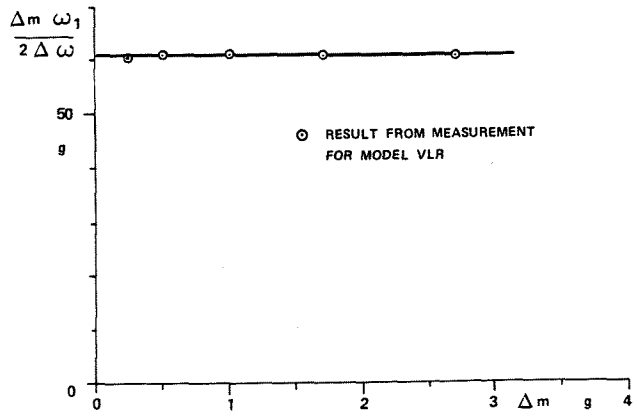

Fig. 6 Determination of generalized mass

6.3 Natural Modes

The AEREL system contains a routine that fits analytic deflecton modes to measured deflection data by the method of least squares. The analytic modes are combinations of products of chordwise and spanwise factors having vanishing second and third order derivatives at the leading and trailing edge and at the wing tip respectively.The first chordwise factor is a constant, the second one is a linear function, and those of higher order resemble the natural modes of a free beam. For the spanwise factor different functions are available. Those chosen for the models tested, which were clamped at the root chord, satisfy this condition.

For wings with control-surfaces, discontinuous functions with the value zero at points off the control-surface can be included. On the control-surface these functions are formed by products of the same kind as those mentioned above, but two of the spanwise factors are a constant function and a function with linear variation.

The number of chordwise factors, NC, was chosen equal to 3, which allows chordwise bending of the lowest order, while the number of spanwise factors, NS, was chosen equal to 4. The first two analytic modes for V00 for these values of NC and NS are compared to the measured values in Fig. 7 and 8 while Fig. 9 and 10 show corresponding results for V00V. The analytic functions are represented by the solid curves and the measured values by circles.

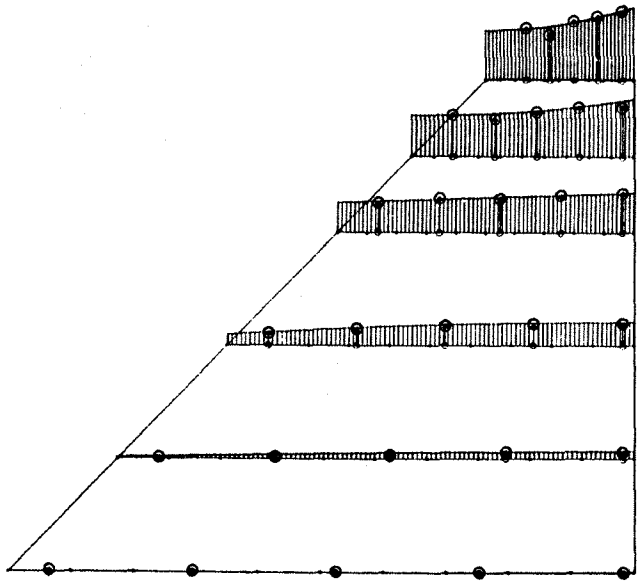

Fig. 7 First mode of V00.

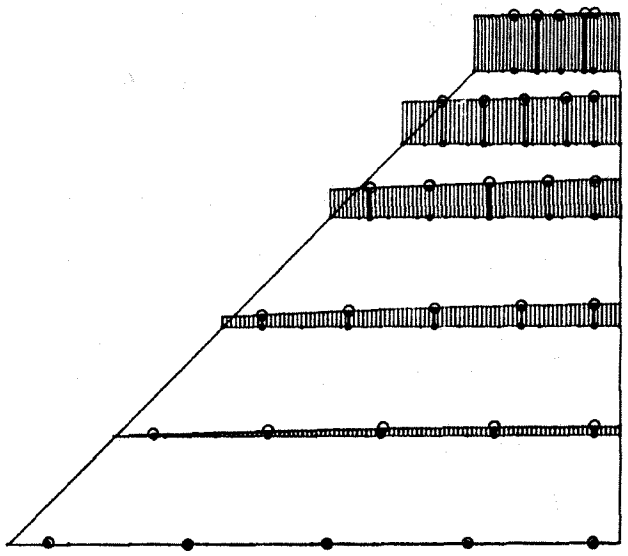

Fig. 9 First mode of V00V.

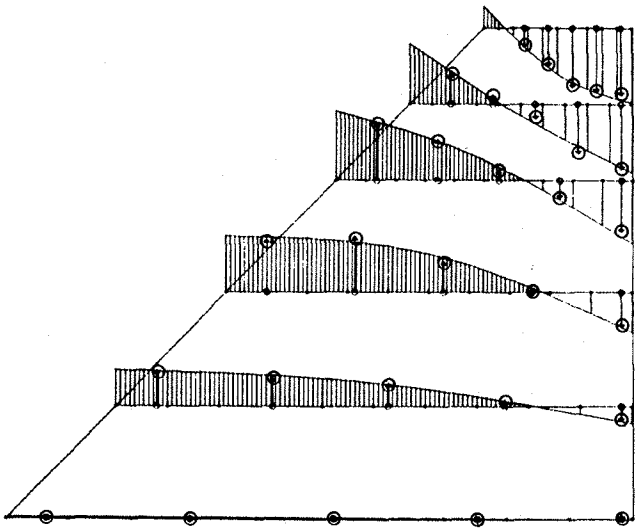

Fig. 8 Second mode of V00.

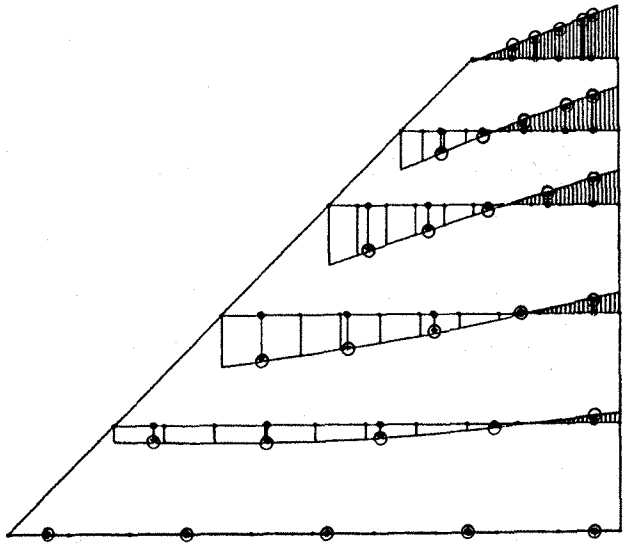

Fig. 10 Second mode of V00V.

In contrast to the analytic modes for V00V, the modes for V00 exhibit on the outboard part of the model a significant amount of chordwise bending. As such a bending can hardly occur at the wing tip for low-order natural modes and as the modes calculated by ASKA agree very well with the analytic modes obtained for V00V (which is only slightly different from V00), it is believed that the analytic modes obtained for V00 are incorrect.

But the analytic modes depend on the measured values and, as the analytic modes were determined in the same way and for the same value of NC for both V00 and V00V, it is concluded that the measured values for V00 are incorrect.

7 GVT RESULTS FOR MODEL FEO

7.1 Natural Frequencies

VFA and ONERA obtained the following values for the natural frequencies from their ground vibration tests:

VFA: 50.5, 86.2, 108.0, 187.3, and 204.7 Hz.
ONERA: 51.3, 85.6, 109.4, 183.3, and 195.7 Hz.

7.2 Generalized Masses

Reduced to modes normalized in the same way, the results for the generalized masses from the two tests are given in Table 4. They are seen to differ significantly in particular for the third mode.

Table 4 Generalized masses for FEO

Source	Mode No 1	2	3	4	5
VFA	0.254	1.328	0.613	0.074	1.270
ONERA	0.238	1.262	1.451	0.062	0.127

7.3 Natural Modes

The first and the second natural modes are first order bending and torsion modes, the fourth and the fith may be said to be second order bending and torsion modes, while the third mode is primarily a rigid flap rotation mode.

The results for the first and the fith mode are shown in Fig. 11 and 12 respectively. A certain disagreement of the shapes defined by the two measurements is noticed.

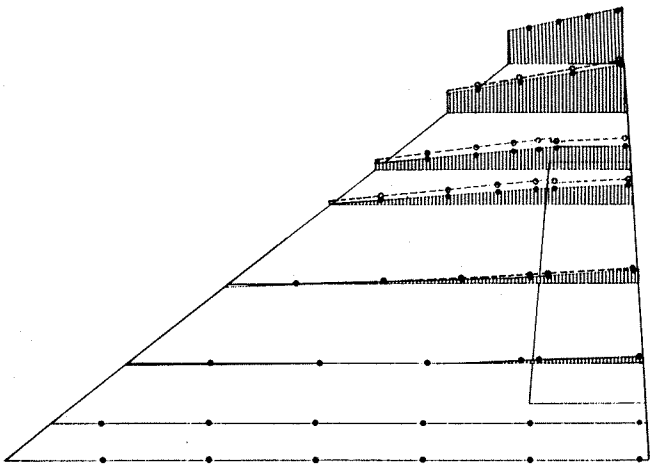

Fig. 11 Comparison of results for the first mode for FEO

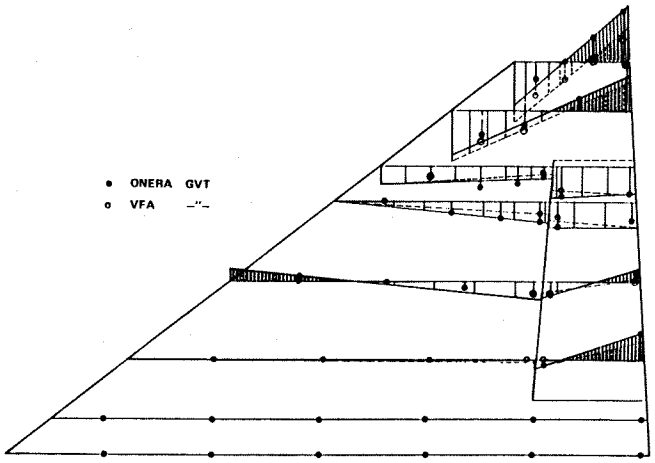

Fig. 12 Comparison of results for the fith mode for FEO

8 AERODYNAMIC CALCULATIONS

The AEREL system contains subprograms for calculation of aerodynamic transfer functions on the basis of the linearized theory. Two of these are the ADE (Advanced Doublet Element) program (Ref. 3) and the CHB (Characteristic Box) program (Ref. 4), which are programs for subsonic and supersonic speeds respectively.

The ADE program is applicable to a nonplanar configuration of trapezoidal wing panels, but this capability was not utilized. The missile model, which has 4 forward fins and 4 rear fins in planes inclined 45 degrees to the wing plane, was treated in a simplified way. The four inboard fins were disregarded since they are inefficient due to the closeness to the launcher and the two pairs of the outboard fins were each considered equivalent to a single fin in the wing plane. This is obtained by rotation of the missile 45 degrees.

Wind tunnel tests or calculations for supersonic Mach numbers for the models with launcher and missile have not been completed.

For the models V00, V00V, and FEO, the aerodynamic transfer functions were calculated both by the programs ADE and CHB, i. e. on the basis of the ordinary linearized theory, and by the so called FP program, which is a finite difference program developed recently at SAAB (Ref. 1). As this program is based on the full potential equation, thickness effects are taken into account.

9 FLUTTER TEST TECHNIQUE

In the flutter tests at VFA, the model was excited solely by the turbulence of the flow and the model response was measured by means of strain gauge sensors at the wing root. An xy-plotter was used for displaying the RMS value of the signal, which was recorded on tape. Frequency and damping values were extracted by means of an HP5423A analyzer, and the flutter-critical density of the flow was determined by extrapolation of a curve through damping values for densities near the critical value.

In the wind tunnel tests at ONERA, response data were recorded and analyzed in a similar way, but eigenvalues were determined for three low-order modes in addition to that for the critical mode. Excitation of the model was achieved by means of the ONERA hydraulic actuator, which was also used in a control loop for flutter suppression in critical cases.

10 FLUTTER CALCULATIONS

The flutter routine of the AEREL system which was used here yields results for the true damping of the natural modes, because it solves the nonlinear eigenvalue problem that results upon Laplace transformation of the equations for general motion (Ref. 5). Newton-Raphson iteration and simple analytic functions approximating the aerodynamic transfer functions are used in this routine (Ref. 6 and 7)

The flutter critical flow variables were determined both at VFA and ONERA by keeping the Mach number at a constant given value and gradually increasing the stagnation pressure while observing the damping.

11 FUTTER RESULTS FOR THE SMALL MODELS

11.1 Model V00

Attemts to calculate the flutter critical free-stream density for the model V00 using the initially obtained GVT data (by the impulse hammer technique) were not successful. The disagreement of the results have been found to be due to the previously disclosed errors in the measured generalized masses and the natural modes. Since it is interesting to show the effects of these errors, the flutter densities obtained on the basis of the erroneous data are illustrated in Fig. 13.

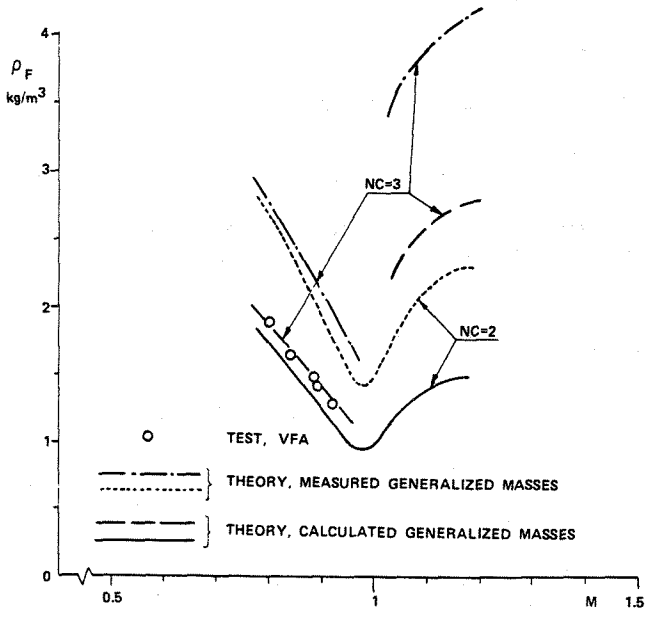

Fig. 13 Effect of inaccurate GVT results on the flutter density of the model V00

Generalized masses for V00 calculated by the AEREL routine for NC equal to 2 (chordwise bending not allowed) and 3 do not differ much from each other and not much from those measured by the Laser Dopler Vibrometer for the model V00V (which is essentially the same as V00).

The difference between the flutter densities for NC = 3 and NC = 2 is therefore due to the difference between the aerodynamic transfer functions, which in turn is due to the chordwise bending and thus to the errors in the measured deflection values. As seen by comparing each of the two curves for NC = 2 to the corresponding one for NC = 3 in figure 13, these errors have a much greater effect in the supersonic range than in the subsonic range.

By comparing the dotted curve to the solid one and the dash-dotted curve to the dashed one, it is also seen that the effect of the inaccuracies of the generalized masses is considerable in both speed ranges. Use of the experimentally determined generalized masses yields unconservative flutter densities.

11.2 Model V00V

Flutter results for the model V00V are shown in Fig. 14 and 15. The shape of the curves for the damping coefficient in the former figure indicate that the flutter instability is of the catastrophic type.

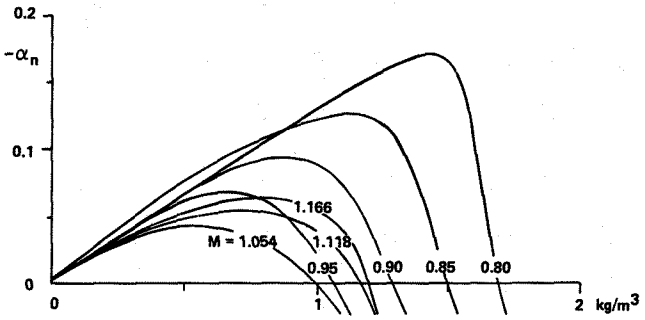

Figure 14 Damping of the critical mode of V00V

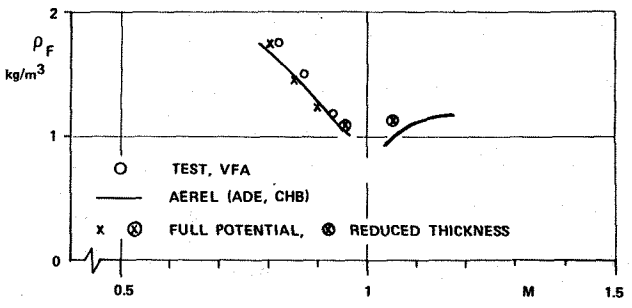

Figure 15 Flutter density for V00V

As seen from Fig. 13 and 15, the experimental results for the flutter density for V00V are nearly the same as those for V00. Hence, the effect of the difference in shape of the model section at the trailing edge does not seem to be significant.

Flutter results calculated on the basis of the linearized aerodynamic theory via the ADE and CHB programs are shown by the solid curves in Fig. 15. They agree very satisfactorily with those from the VFA tests, which have been completed only for subsonic speeds.

The FP program, which takes the effect of the wing thickness into account, should produce the same result for zero thickness as a program based on the linearized theory. It was decided to check this by applying the FP program to the model V00V which has a maximum relative thickness of about 1 percent at the root and about 5 percent at the tip. The slope of the model section has discontinuities, however, and due to these, acceptable results could not be obtained from the FP program for Mach numbers above 0.9 for the true section. Calculations by the FP program for the higher Mach numbers were therefore performed for the thickness reduced to a value less than one percent at all stations.

The expectation that the full potential theory and the linearized theory yield the same result for vanishing thickness is seen to be supported by the results obtained.

11.3 Model VLR

Theoretical results for the eigenvalues and the damping coefficient for the flutter critical mode of the model VLR, the model with launcher and missile, are illustrated in Fig. 16.

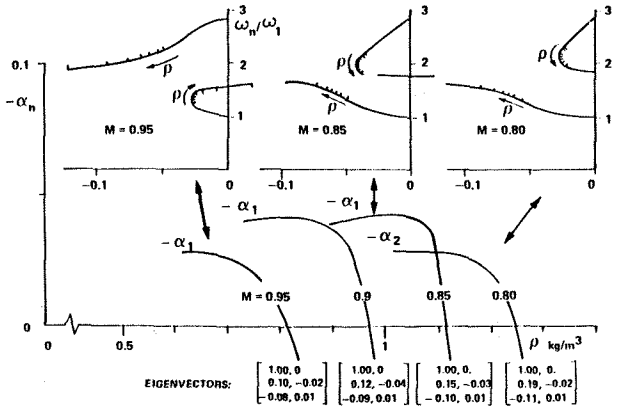

Fig. 16 Damping of the critical mode of VLR

Eigenvectors associated with the critical mode for the Mach numbers considered are also shown in the figure and it is seen from them that the flutter mode is essentially a combination of the first bending and the first torsion mode.

As the slope of the damping curves is very steep, the catastrophic nature of the flutter instability seems more pronounced for VLR than for V00 or V00V.

The three smaller diagrams included in Fig. 16 show that the eigenvalues for Mach numbers less than about 0.9 and those for greater Mach numbers move in different ways in the complex frequency plane.

11.4 Models VLRF And VLRB

Theoretical and experimental results for the flutter density are shown in Fig. 17 for VLR, VLRF, and VLRB.

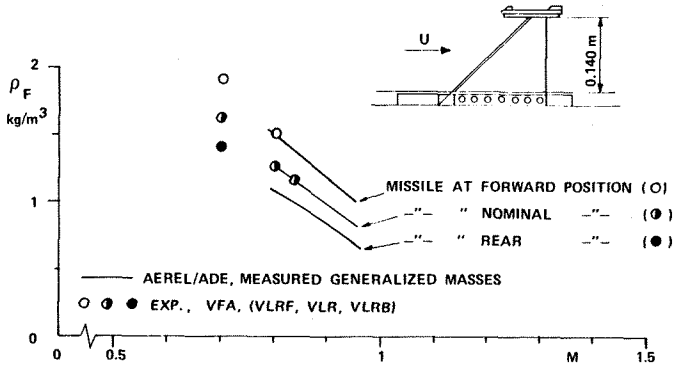

Fig. 17 Flutter density for missile at different positions

As seen, the agreement between the measured and calculated flutter densities is very good and the calculated effect of moving the missile agrees with the experimental prediction too. A more forward location yields a higher flutter density.

11.5 Models VLRUFF, VLRUFB, VLRUF

The effect on the flutter density of discarding the aerodynamic forces on the missile fins partly or completely was studied theoretically. The forward fins were removed in one case, the rear fins in a second, and all fins in a third case, which implies neglecting the aerodynamic forces since the fins have very small masses compared to the mass of the missile body.

The results are compared in Fig. 18 to the experimental and theoretical results for VLR, i. e. for the model with all fins retained. Removal of the forward fins is seen to increase the flutter density while removal of the rear fins reduces it.

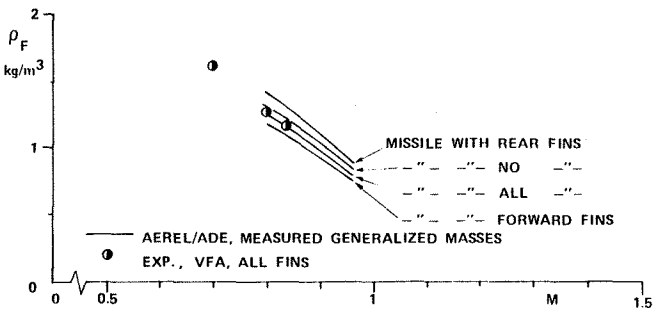

Fig. 18 Flutter density for different fin arrangements

11.6 Model VLT

The calculated results for the different fin arrangements have been checked experimentally only in one case, namely, in the case of a missile with no fins. As shown by Fig. 19, close agreement was again obtained.

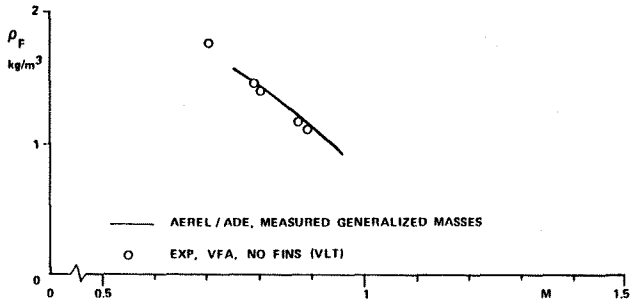

Fig. 19 Flutter density for model VLT

12 FLUTTER RESULTS FOR THE MODEL FEO

Flutter calculations have been performed on the basis of modes, frequencies, and generalized masses from both the VFA GVT and the ONERA GVT. Five modes were determined in the tests and all five modes were used in the approximation to the elastic deflection of the model.

Aerodynamic transfer functions were calculated by the ADE and CHB programs for 10 reduced frequencies and 8 Mach numbers, and functions of the Jones type and of the kind proposed in Ref. 7 were fitted to the calculated values for subsonic and supersonic flow respectively.

The same procedure and flutter routine were used in calculations based on aerodynamic transfer functions from the FP program.

12.1 Results Based On Linearized Theory

The stagnation temperature, which did not vary much during the tests, was taken equal to 305 degrees K in the calculations. Like the tests, these were performed for each Mach number by increasing the stagnation pressure in small steps. The results obtained for the damping coefficient for the first four modes for a stagnation pressure of 1.5 bar are plotted in Fig. 20-23.

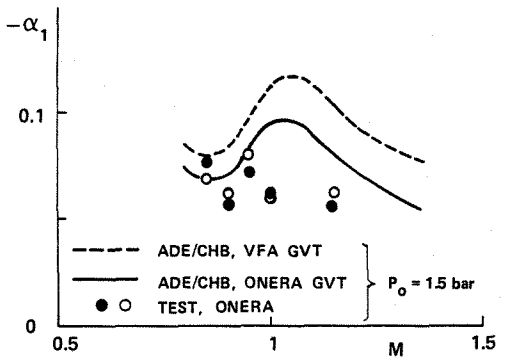

Fig. 20 Damping of the first mode of FEO

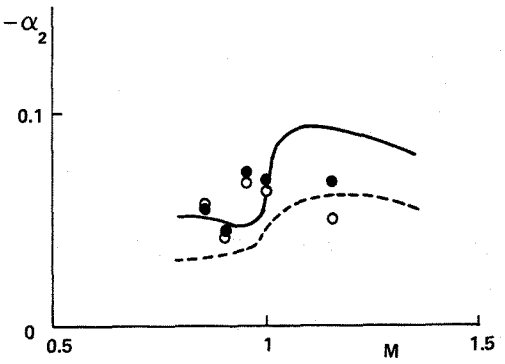

Fig. 21 Damping of the second mode of FEO

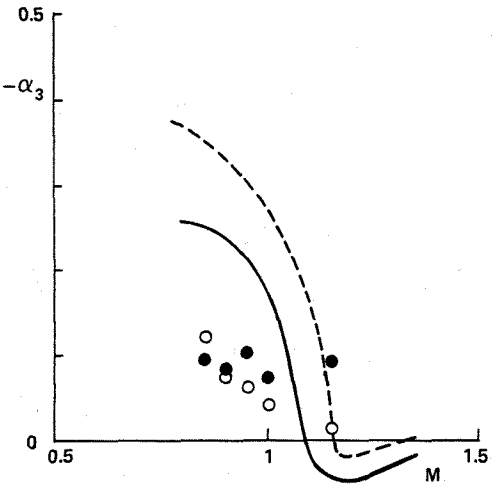

Fig. 22 Damping of the third mode of FEO

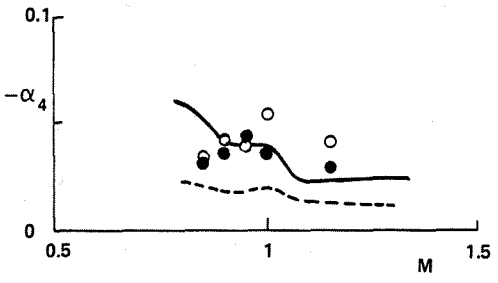

Fig. 23 Damping of the fourth mode of FEO

The solid and the dashed curves in the figures represent results calculated on the basis of data from the GVT:s by ONERA and VFA respectively, while the circles represent damping values measured by ONERA in the flutter tests.

Results from tests for two different configurations have been included in the figures where they are represented by open and filled circles. The two sets of results were included because it yields increased confidence in the measured values. The difference between the configurations, which is due to removal of a small part of the flap with small mass, should have only a small effect on the results. It increased the natural frequency of the third mode by 8 percent.

The frequency part of the eigenvalues obtained are given by the frequency ratios shown in Fig. 24-27; the reference frequency, ω_r, is equal to the natural frequency (in still air) for the first mode.

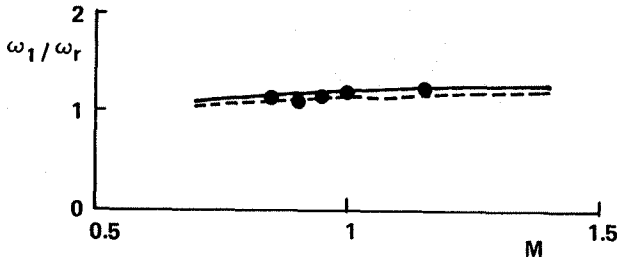

Fig. 24 Frequency of the first mode of FEO

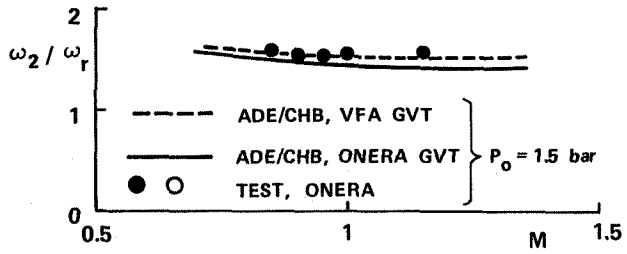

Fig. 25 Frequency of the second mode of FEO

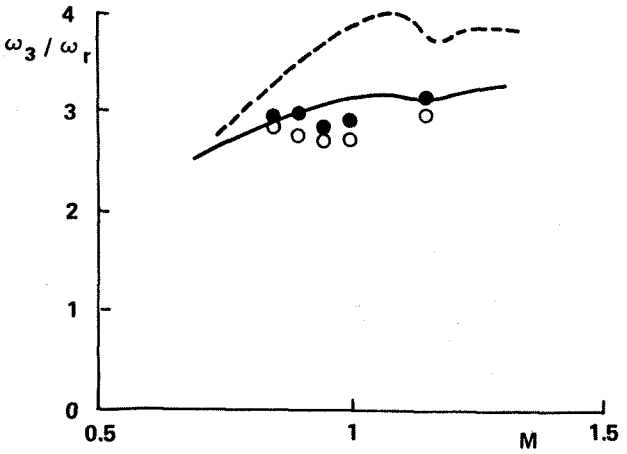

Fig. 26 Frequency of the third mode of FEO

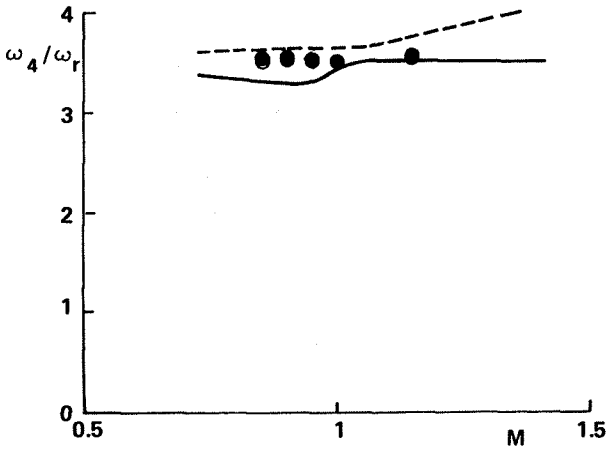

Fig. 27 Frequency of the fourth mode of FEO

The instability that barely tends to appear, as seen from Fig. 22, for this model for the stagnation pressure mentioned is a mild type of flutter, whereas the flutter of the small models was of the catastrophic type. Therefore, we have to consider the damping coefficients instead of the flutter critical density in the comparisons and anticipate due to this greater deviations. It is more difficult, namely, to predict these coefficients, both experimentally and theoretically, than the critical density for catastrophic flutter.

Neither of the two theoretical predictions, which are shown in Fig. 20-23, is in perfect agreement with the experimental results, but, with regard to the difficulty of determining the damping coefficients, the theoretical and the experimental results are surprisingly close to each other. It is seen that the accuracy of the GVT results is important for the comparison and that data from the ONERA test yield somewhat better agreement.

In a limited supersonic range, the theoretical predictions are conservativ and predict a weak instability. This is at least partly due to the well known fact that the imaginary part of the aerodynamic flap moment due to flap rotation, as predicted by both the linearized theory and the full potential theory, is negative in a reduced frequency range for low-supersonic Mach numbers.

12.2 Results Based On FP Theory

Results for the damping coefficients from a flutter calculation based on aerodynamic forces from the full potential program (Ref. 1) and GVT data from the VFA test are shown in Fig. 28-30. They are compared there to results from a corresponding calculation based on the linearized theory and the same GVT data. The kind of the analytic expression employed for representing the natural modes was likewise the same, but different from the kind used for the results in Fig. 20-27 (less accurate for high order modes).

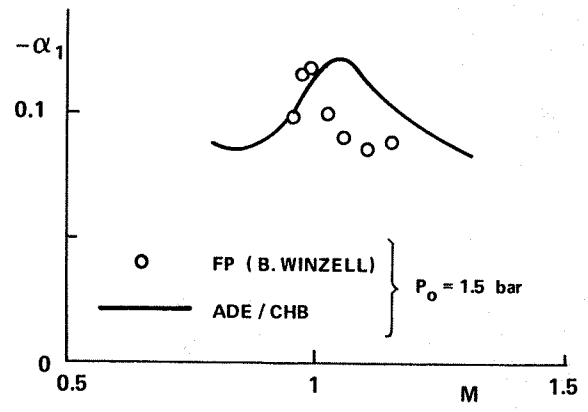

Fig. 28 Damping of the first mode of FEO

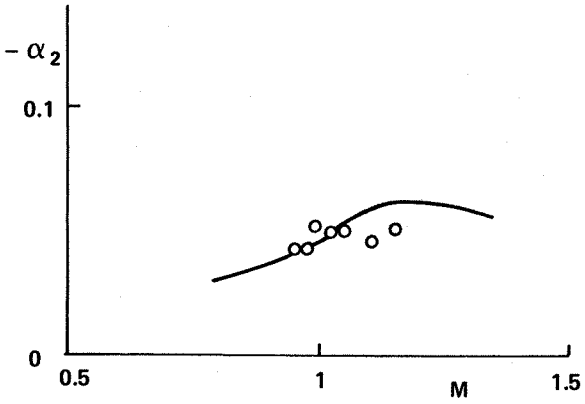

Fig. 29 Damping of the second mode of FEO

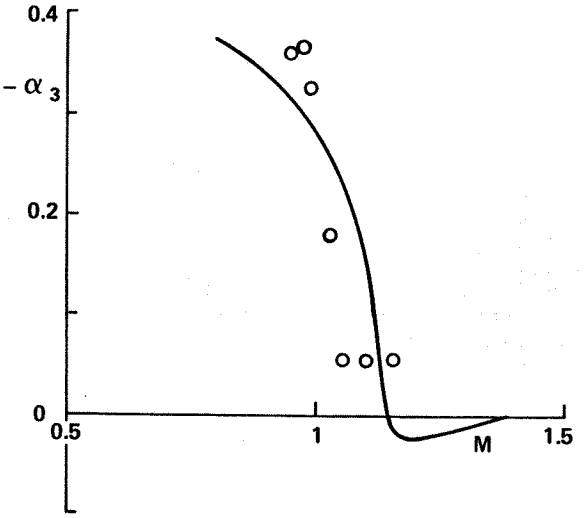

Fig. 30 Damping of the third mode of FEO

This comparison shows that the FP theory yields essentially the same results as the linearized theory for the model FEO, which, like the small models, is thin and was tested at zero incidence.

13 CONCLUSIONS

A number of small and thin semispan wing models, which in some cases have a launcher and a missile at the tip, and a much larger model, which is likewise thin and has a trailing edge flap, have been subjected to ground vibration tests and flutter tests at zero incidence in a small and a large wind tunnel respectively. Based on data from the ground vibration tests, flutter calculations using mainly linearized aerodynamic theory have been performed and the results have been compared to those from the experiments.

The agreement between the theoretical and the experimental results for the flutter critical flow density for the small models (including those with missile at the tip) is close, and that for the damping coefficients for the large model is not quite as close but satisfactory for flutter prevention.

It is thus concluded that the linearized aerodynamic theory is satisfactory for flutter prevention of thin wings at zero incidence.

As expected for thin wings at zero incidence, calculations for two of the models on the basis of aerodynamic forces from the full potential theory were not found to produce results significantly different from those based on the linearized theory.

In order to evaluate the validity of unsteady aerodynamic theories and computer programs, it is necessary to prove that the experimental results employed in each case for comparison are accurate, which has been done here as far as possible.

14 ACKNOWLEDGEMENT

The Swedish Defence Administration and SAAB financed this investigation, R. Frankmark and L. Sundberg at VFA, B. Åkerlindh and several others at SAAB, and R. Destuynder and A. Gravelle at ONERA contributed to the experimental part, B. Winzell performed FP calculations, and I-L Mattsson drew the figures, which is all gratefully acknowledged.

15 REFERENCES

1 Winzell B.,"An Unsteady Full Potential Equation Solver for 3-D Wings," SAAB Report TKLF-0-87:23, April, 1987.
2 Halvorsen W.G and Brown D.L,"Impulse Technique for Structural Frequency Response Testing," Sound and Vibration,November 1977, p. 8-21.
3 Stark V.J.E.,"The Advanced Doublet Element Method," (to be published)
4 Stark V.J.E.,"Calculation of Aerodynamic Forces on Two Oscillating Finite Wings at Low Supersonic Mach Numbers," SAAB TN 53, February, 1964.
5 Stark V.J.E.,"General Equations of Motion for an Elastic Wing and Method of Solution," AIAA J., Vol. 22, No. 8, August 1984, P. 1146-1153.
6 Stark V.J.E.,"A Flutter Eigenvalue Program Based on the Newton-Raphson Method," AIAA J., Vol. 22, No. 7, July 1984, p. 993-995.
7 Stark V.J.E.,"Flutter Calculation by a New Program," Proc. DGLR Symposium on Aeroelasticity and Structural Dynamics, April 1-3, Aachen, 1985. DGLR-Bericht 85-02, p. 276.